GEOMETRIC CONTROL APPROACH FOR THE FOUCAULT PENDULUM

Alfonso Anzaldo-Meneses
Basic Sciences Department
UAM-Azcapotzalco
Av. San Pablo 100, Azcapotzalco
02200 México D.F.
answald@ymail.com

Felipe Monroy-Pérez
Basic Sciences Department
UAM-Azcapotzalco
Av. San Pablo 100, Azcapotzalco
02200 México D.F.
fmp@correo.azc.uam.mx

Abstract

Non-linear control systems defined by means of distributions of smooth vector fields are relevant, partly because they provide good models for nonholonomic systems in mechanics, automation and classical particles. In this paper we approach the classical Foucault pendulum, which is accepted as indisputable demonstration of the Earth's rotation movement, through the formalism of geometric control theory. By applying the Pontryagin Maximum Principle, we derive some geometric properties for trajectories for the case of small oscillations, we establish also a link of the Foucault pendulum with the well known Hopf fibration, which is a ubiquitous geometric object in physics.

Key words

Foucault pendulum, geometric control, Pontryagin principle, Hopf fibration.

1 Introduction

The experiment of the Foucault pendulum goes back to 1851 and is recognized as a feasible demonstration of Earth's rotation movement. In this paper we approach the system that models the experiment through the framework of the geometric optimal control theory, restricting ourselves to small oscillations and the symmetric case in the sense that we shall explain latter. We write the equations as an optimal control system on a three dimensional manifold and apply the Pontryagin Maximum Principle to derive some geometric properties of the solutions.

Geometric non-linear control theory merges differential geometric techniques with the analysis of different aspects of non-linear control systems, including equilibria, stabilization, and optimal control problems. The foundations of the theory goes back to the early seventies with the pioneering papers by C. Lobry, [C. Lobry, 1970], R.W. Brockett [R.W. Brockett, 1972], and H.Sussmann and V. Jurdjevic [V. Jurdjevic, H.J. Sussmann,1972], among others.

The theory has been especially successful in applications to certain problems in geometric mechanics [F. Bullo, A.D. Lewis, 2004] and robotics [R. Murray, L. Zexiang,S.S. Sastry, 1994]. There is an extensive literature presenting the general theory of geometric nonlinear control systems, we refer the reader to the volume by V. Jurdjevic [V. Jurdjevic, 1997] and the recent book by A. Agrachev and Y. Sachkov [A. Agrachev, Y.L. Sachkov, 2004].

Geometric Optimal control for non-linear systems finds its origin in the well-known Pontryagin Maximum Principle (PMP), originally published in the book [L.S. Pontryagin, V.G. Boltyanskii, R.V. Gamkrelidze; E.F. Mishchenko, 1962]. This important result and its subsequent generalizations provide natural extensions of the necessary conditions for optimality stated in the classical calculus of variations, see for instance [M. Giaquinta, S. Hildebrandt, 1996], and has recently lead to new geometry that goes in the literature under the name of Sub-Riemannian or Carnot-Caratheodory geometry.

Generally speaking a sub-Riemannian (s-R) structure on a manifold $\mathcal{M}$ is determined by a completely non-integrable (non-holonomic) distribution Δ of smooth vector fields, together with a smooth metric defined on Δ. An absolutely continuous curve α is $\Delta-$admissible if $\dot{\alpha}(t) \in \Delta(\alpha(t))$ for almost all t. The s-R distance between two points $p, q \in \mathcal{M}$ is realized by the minimum of the length of all $\Delta-$admissible curves connecting p and q. In is known that the s-R geodesic problem can be formulated as an optimal control problem on $\mathcal{M}$, in this paper we shall pursue the latter approach, for details about the former, we refer the reader to excellent survey by A.M. Vershik et al. [A.M. Vershik and V. Ya. Gershkovich, 1991], the volume by R. Montgomery [R. Montgomery, 2002], and the recent book by O.Calin et al. [O. Calin, D.Ch. Chang, 2009].

An optimal control problem on connected n-

dimensional smooth manifold $\mathcal{M}$, can be given by means of a rank $k < n$ distribution of vector fields $\Delta \subset T\mathcal{M}$. The iteration of the Lie bracket of vector fields in Δ yields the following flag of modules of vector fields:

$$\Delta^1 \subset \Delta^2 \subset \cdots \subset \Delta^l \cdots \subset T\mathcal{M},$$

where $\Delta^1 = \Delta$ and $\Delta^{i+1} = \Delta^i + [\Delta, \Delta^i]$. The distribution is said to be *bracket generating*, if for each $m \in \mathcal{M}$, there exist a positive integer l for which $\Delta^l_m = T_m\mathcal{M}$. The growth vector of Δ at m is defined as $(n_1, \ldots, n_l)$, where $n_j(m) = \dim(\Delta^j_m)$, the distribution is said to be *regular* if the growth vector is independent of the base point.

A regular, bracket generating distribution $\Delta = \{X_1, \ldots, X_k\}$ determines the following driftless control-affine system

$$\dot{q} = u_1 X_1(q) + \cdots + u_k X_k(q), \tag{1}$$

where $t \mapsto \mathbf{u}(t) = (u_1(t), \ldots, u_k(t))$, the admissible control, is bounded and measurable.

An absolutely continuous curve $t \mapsto q(t),\ t \in [0, T_q]$ is said to be admissible is $\dot{q}(t) \in \Delta(q(t)),\ a.e.$, that is, there is an admissible control $\mathbf{u}$ such that (1) holds.

For a continuous cost $c(x, \mathbf{u})$ one can consider the functional

$$\mathcal{E} = \int_0^{T_q} c(x, \mathbf{u}), \tag{2}$$

to have at the end, the optimal control problem on $\mathcal{M}$ of finding, among the solutions $t \mapsto (q, \mathbf{u})$ of (1) the one that minimizes (2).

Apart from this introduction this paper contains three sections and an appendix. In section 2 we present the standard mathematical model for the Foucault the pendulum. In section 3, under certain considerations for small oscillations, we formulate the Foucault pendulum as an optimal control problem an a smooth manifold, for this problem we apply the PMP and derive some geometric properties of the solutions. In section 4 we establish a natural connection of the trajectories of the problem to the well known Hopf fibration. At the end, in section 5 we derive some conclusions and discuss further research perspectives. The appendix includes some technical details of the Foucault pendulum that is in the process of being installed at the Universidad Autónoma Metropolitana-Azcapotzalco in México City. It is fair to recognize that our involvement in the project of installation of the Foucault pendulum, has been one of our sources of motivation for studying it theoretically under new perspectives.

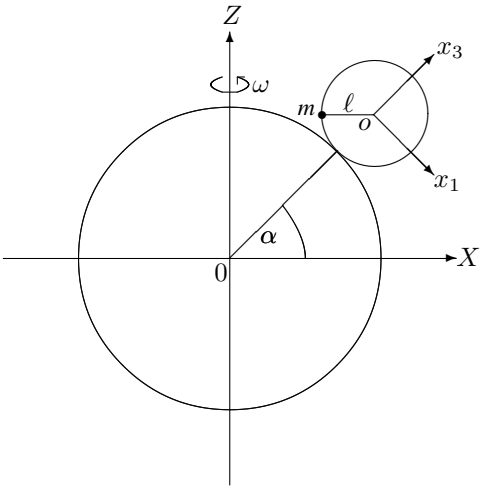

Figure 1. Pendulum at geographic latitude α

2 The standard model for the Foucault pendulum

We take and inertial frame with coordinates (X, Y, Z), and a pendulum of length ℓ and point mass m, oscillating taking into consideration Earth's rotation movement. The angular velocity of the rotation is denoted as $\vec{\omega}$, and the mass' position is measured from a fixed coordinate system with origin located at latitude α and coordinates (x_1, x_2, x_3), the x_1 direction on a meridian great circle in north-south sense, the x_2 direction on a latitude circle in west-east sense and the x_3 direction perpendicular to the tangent plane at the intersection of both circles as illustrated in figure 1.

A vector $\vec{r}$ in the non-inertial system on Earth's surface behaves as

$$\frac{d\vec{r}}{dt} = \dot{\vec{r}} + \vec{\omega} \times \vec{r},$$

where $\dot{\vec{r}} = (\dot{x}, \dot{x_2}, \dot{x_3})$ and $\vec{\omega} = (-\omega \cos\alpha, 0, \omega \sin\alpha)$, with $\omega \approx 10^{-4}$ sec^{-1}. The kinetic energy is given as follows

$$\frac{m}{2}\left|\frac{d\vec{r}}{dt}\right|^2 = \frac{m}{2}(|\dot{\vec{r}}|^2 + |\vec{\omega} \times \vec{r}|^2 + 2\dot{\vec{r}} \cdot (\vec{\omega} \times \vec{r})\,).$$

The second term leads to a centrifugal force perpendicular to the rotation axis and can be disregarded. For the third term we observe that

$$\begin{aligned}
&\dot{\vec{r}} \cdot (\vec{\omega} \times \vec{r}) = \vec{\omega} \cdot (\vec{r} \times \dot{\vec{r}}) \\
&= \omega_{x_1}(x_2\dot{x_3} - x_3\dot{x_2}) + \omega_{x_2}(x_3\dot{x_1} - x_1\dot{x_3}) \\
&+\omega_{x_3}(x_1\dot{x_2} - x_2\dot{x_1}),
\end{aligned}$$

finally we also have to take into account the following holonomic constraint

$$\delta x_1^2 + x_2^2 + x_3^2 - \ell^2 = 0, \tag{3}$$

where δ is a dimensionless asymmetry parameter due to different moments of inertia or some other asymmetries of the experiment, for details see [A. Anzaldo-Menenses, F. Monroy-Pérez, 2010].

Taking all these constraints into consideration, we have that the complete functional is written as follow:

$$\begin{aligned}\mathcal{S} = \int \Big(& (\frac{m}{2}(\dot{x_1}^2 + \dot{x_2}^2 + \dot{x_3}^2 - 2gx_3) \\ & + \lambda_0(\delta x_1^2 + x_2^2 + x_3^2 - \ell^2) \\ & + \lambda_1(\dot{\xi}_1 + x_2\dot{x_3} - x_3\dot{x_2}) \\ & + \lambda_2(\dot{\xi}_2 + x_3\dot{x_1} - x_1\dot{x_3}) \\ & + \lambda_3(\dot{\xi}_3 + x_1\dot{x}_2 - x_2\dot{x}_1)\Big)\, dt,\end{aligned}$$

where λ_0 Lagrange parameter and $\lambda_1 = -m\omega\cos\alpha$, $\lambda_2 = 0$ and $\lambda_3 = m\omega\sin\alpha$, (the last differentials do not alter the Euler-Lagrange equations for $\vec{r}$). The λ_i can be taken as the Lagrange parameters associated with the nonholonomic constraints

$$\omega_1 = d\xi_1 + x_2dx_3 - x_3dx_2 = 0, \tag{4}$$
$$\omega_2 = d\xi_2 + x_3dx_1 - x_1dx_3 = 0, \tag{5}$$
$$\omega_3 = d\xi_3 + x_1dx_2 - x_2dx_1 = 0, \tag{6}$$

which is tantamount of saying that the $\omega_i's$ are constants, since the $\xi_i's$ are cyclic variables.

3 Optimal control approach for the Foucault pendulum

We consider the Lagrangian

$$\begin{aligned}L_0 = & \frac{m}{2}(\dot{x}_1^2 + \dot{x}_2^2 + \dot{x}_3^2) - mgx_3 \\ & + \lambda_1(\dot{\xi}_1 + x_2\dot{x}_3 + x_3\dot{x}_2) \\ & + \lambda_2(\dot{\xi}_2 + x_3\dot{x}_1 + x_1\dot{x}_3) \\ & + \lambda_3(\dot{\xi}_3 + x_1\dot{x}_2 + x_2\dot{x}_3),\end{aligned}$$

subject to constraint (3).

The last three terms of the Lagrangian result from the fact that the pendulum is in a non-inertial coordinates system. Equivalently, we can take the Lagrangian

$$L = \frac{m}{2}(\dot{x}_1^2 + \dot{x}_2^2 + \dot{x}_3^2) - mgx_3,$$

subject to the non-holonomic constraints (4), (5)and (6).

For a standard Foucault pendulum only small oscillations are important, therefore $\dot{x}_3 \simeq 0$ and, from the holonomic constraint we have

$$x_3 = \sqrt{\ell - x_1^2 - \delta x_1^2} \simeq \ell - \frac{1}{2\ell}(\delta x_1^2 + x_2^2),$$

so that the Lagrangian reduces to

$$L = \frac{m}{2}(\dot{x}_1^2 + \dot{x}_2^2) - \frac{mg\delta}{2\ell}x_1^2 - \frac{mg}{2\ell}x_2^2$$

together with the non-holonomic constraint

$$\dot{\xi} = x_1\dot{x}_2 - x_2\dot{x}_1. \tag{7}$$

The problem can now be formulated as the optimal control problem of minimization of the functional

$$\int c(x, \dot{x})dt, \tag{8}$$

with

$$c(x, \dot{x}) = \frac{m}{2}(\dot{x}_1^2 + \dot{x}_2^2) - \frac{m\omega_1}{2}x_1^2 - \frac{m\omega_2}{2}x_2^2,$$

and $\omega_1 = \sqrt{g\delta/\ell}, \omega_0 = \sqrt{g/\ell}$, amongst the admissible solutions of the following control affine system

$$\frac{dq}{dt} = u_1X_1(q) + u_2X_2(q), \tag{9}$$

with

$$\begin{aligned}X_1 &= \frac{\partial}{\partial x_1} - x_2\frac{\partial}{\partial \xi} \\ X_2 &= \frac{\partial}{\partial x_2} + x_1\frac{\partial}{\partial \xi}\end{aligned}$$

The state variable is three-dimensional $q = (x_1, x_2, \xi)^t$, and the velocities are taken as control parameters, that is,

$$u_1 = \dot{x}_1, u_2 = \dot{x}_2.$$

we assume further that $\mathbf{u} = (u_1, u_2)$ is measurable and bounded.

3.1 The Pontryagin Maximum Principle

The distribution $\Delta = \{X_1, X_2\}$ is bracket generating, regular and generates a three dimensional step-2 nilpotent Lie algebra with the only non-zero bracket X_3 given by

$$X_3 = [X_1, X_2] = 2\frac{\partial}{\partial \xi},$$

In fact, we have a Lie algebra isomorphic to the Heisenberg Lie algebra, and the manifold $\mathcal{M}$ is the Heisenberg group.

Necessary conditions for admissible optimal trajectories of the above optimal control problem are given by the PMP that we now roughly explain, for details see for instance [V. Jurdjevic, 1997].

The cotangent bundle $T^*\mathcal{M}$ is a symplectic manifold with canonical symplectic form Ω, that allows to associate to each smooth function $H : T^*\mathcal{M} \to \mathbb{R}$, a Hamiltonian vector field $\vec{H}$, according to the expression $dH_\eta(v) = \Omega(v, \vec{H}(\eta))$, where $v \in T_\eta T^*\mathcal{M}$ and $\eta \in T^*\mathcal{M}$. For then the Hamiltonian flow $t \mapsto (g(t), p(t))$ obeys the so-called Hamilton equations

$$\frac{dg}{dt} = (dL_g)(dH) \tag{10}$$

$$\frac{dp}{dt} = -(ad^* dH)(p), \tag{11}$$

her $g \mapsto L_g$ denotes the left translation.

We consider the corresponding Hamiltonians (momenta) $H_i's$ associated to the vector fields $X_i's$, i.e. $p(X_i) = H_i$. The coordinates on the cotangent bundle are (x_1, x_2, H_1, H_2) and the algebra for the H_i' is enlarged (see for example Abraham, R. & Marsden, J.E. 1987, Foundations of Mechanics, Addison-Wesley.) according to

$$\{x_i, x_j\} = 0, \quad \{x_i, H_j\} = X_j(x_i).$$

The commuting relations for the step-2 nilpotent Lie-Poisson algebra generated by the Hamiltonians and the coordinates functions is summarized in the following table

$\{\cdot,\cdot\}$	H_1	H_2	x_1	x_2
H_1	0	H_3	-1	0
H_2	$-H_3$	0	0	-1
x_1	1	0	0	0
x_2	0	1	0	0

Table 1

A control dependent Hamiltonian is written as follows

$$\begin{aligned}\mathcal{H}_{\lambda_0,\mathbf{u}} &= -\lambda_0 c(x,u) + p(u_1 X_2(q) + u_2 X_2(q)) \\ &= -\lambda_0 c(x,u) + u_1 H_1 + u_2 H_2,\end{aligned}$$

as customary, λ_0 is normalized to take the values 1 or 0, the integral curves of the Hamiltonian system associated to $\mathcal{H}_{\lambda_0,\mathbf{u}}$ are called extremals, the ones corresponding to 1 are called normal, whereas those corresponding to 0 are called abnormal, we restrict ourselves to the normal case, PMP then read as follows:

Theorem 3.1. *A solution curve $t \mapsto (x(t), \widehat{\mathbf{u}})$ is optimal if it is the projection of an extremal curve (x, p) along which the inequality $\mathcal{H}_{\lambda,\widehat{\mathbf{u}}} \geq \mathcal{H}_{\lambda,\mathbf{w}}$ holds a.e., for all $\mathbf{w} \in \mathcal{U}$.*

The maximality condition readily implies that along extrema $mu_i = H_i$, therefore the system Hamiltonian becomes quadratic

$$\mathcal{H} = \frac{1}{2m}(H_1^2 + H_2^2) + \frac{m\omega_1}{2}x_1^2 + \frac{m\omega_2}{2}x_2^2.$$

The differential system for the adjoint variable is written by Poisson bracketing as follows:

$$\begin{aligned}\dot{H}_1 &= \{H_1, \mathcal{H}\} = H_2 H_3 - m\omega_1 x_1, \\ \dot{H}_2 &= \{H_2, \mathcal{H}\} = -H_1 H_3 - m\omega_0 x_2, \\ \dot{H}_3 &= \{H_3, \mathcal{H}\} = 0,\end{aligned}$$

from where we can perform a straightforward integration process.

Remark 3.1. *In general, following the same lines, we observe that in the same way, the* PMP *can be applied to more general problems with Lagrangians written as $c(x, \dot{x}) = T(\dot{x}) - V(x)$, subject to non-holonomic constraints.*

4 Foucault pendulum and the Hopf fibration

As it is shown in our previous work [A.Anzaldo-Meneses and F. Monroy-Pérez, 2009], for a symmetric pendulum $\delta = 1$, the solution can be better written by introducing the complex variable $u = x_1 + ix_2$, from where $\dot{\xi}_3 = \mathrm{Im}\,(u\dot{u}^*)$ and $\ddot{u} = -i\frac{2\lambda_3}{m}\dot{u} - \frac{g}{\ell}u$. It follows that

$$u = e^{-i\tilde{\omega}t}(A_+ e^{i\tilde{\omega}_0 t} + A_- e^{-i\tilde{\omega}_0 t}), \tag{12}$$

$$\dot{u} = i\, e^{-i\tilde{\omega}t}(\alpha_+ A_+ e^{i\tilde{\omega}_0 t} + \alpha_- A_- e^{-i\tilde{\omega}_0 t}), \tag{13}$$

$$\begin{aligned}\xi_3 = &-(\alpha_+|A_+|^2 + \alpha_-|A_-|^2)\, t \\ &-2\Re\Big(A_+ A_-^*\,(e^{2i\,\tilde{\omega}_0\, t} - 1)\Big).\end{aligned}$$

For the first two relations, this is a rotation given by the slow mode, with frequency $\tilde{\omega}$, of the fast mode motion, with frequency $\tilde{\omega}_0$. Therefore, the trajectory in base space performs a precession with frequency

$\omega \sin(\alpha)$, whereas ξ_3 increases by the same amount after $2\pi/\tilde{\omega}_0$ where $\tilde{\omega}_0 = \sqrt{\tilde{\omega}^2 + \omega_0^2}$, $\omega_0 = \sqrt{g/\ell}$ and $\tilde{\omega} = \lambda_3/m$. Here, $\tilde{\omega}$ is equal to the rotation angular speed ω times the sinus of the geographical latitude, and the $A_\pm$ depends on he initial conditions. The conservation of energy reads now as follows

$$2H/m = |\dot{u}|^2 + \omega_0^2 |u|^2. \tag{14}$$

For instance, for the original Foucault experimental setting one has, $x_1(0) = R\cos\beta$, $x_2(0) = R\sin\beta$, with $\beta \in (0, 2\pi)$, and $\dot{x}_1(0) = 0$ and $\dot{x}_2(0) = 0$, the trajectories are written as follows:

$$\begin{aligned}
x_1 &= R\cos(\tilde{\omega}t - \beta)\cos(\tilde{\omega}_0\, t) \\
&\quad + \frac{R\tilde{\omega}}{\tilde{\omega}_0}\sin(\tilde{\omega}t - \beta)\sin(\tilde{\omega}_0\, t), \\
x_2 &= -R\sin(\tilde{\omega}t - \beta)\cos(\tilde{\omega}_0\, t) \\
&\quad + \frac{R\tilde{\omega}}{\tilde{\omega}_0}\cos(\tilde{\omega}t - \beta)\sin(\tilde{\omega}_0\, t), \\
\xi_3 &= \frac{R^2\,\tilde{\omega}\,\omega_0^2}{\tilde{\omega}_0^2}\left(\frac{t}{2} - \frac{\sin(2\tilde{\omega}_0\, t)}{4\tilde{\omega}_0}\right).
\end{aligned}$$

Observe that the expressions for x_1 and x_2 are a rotation by an angle $\alpha = \tilde{\omega}t - \beta$ of the ellipse given by the vector

$$(R\cos(\tilde{\omega}_0\, t), \frac{R\tilde{\omega}}{\tilde{\omega}_0}\sin(\tilde{\omega}_0\, t)).$$

This vector has initial value $(R, 0)$ and takes the same value at times $t_k = \pi\, k/\tilde{\omega}_0$, for k integer. Since $\tilde{\omega} < \tilde{\omega}_0$, the nearest approach to the origin is at distance $R\tilde{\omega}/\tilde{\omega}_0$. The curves in base space are hypocycloids.

We establish now the connection of these solutions with the well know Hopf fibration, we restrict ourselves to the symmetric pendulum, that is $\delta = 1$.

As is well known, the Hopf fibration describes the unit three dimensional sphere $\mathbb{S}^3$ by means of circles $\mathbb{S}^1$ and the two dimensional sphere $\mathbb{S}^2$. It was shown by H. Hopf himself [H. Hopf , 1931], that a many to one continuous function from the $\mathbb{S}^3$ onto $\mathbb{S}^2$, can be defined in such a way that distinct points of $\mathbb{S}^2$ come from a distinct circles of $\mathbb{S}^3$, so that $\mathbb{S}^3$ is fibered by circles for each point of $\mathbb{S}^2$. In modern notation it is customary to denote this bundle structure as follows

$$\mathbb{S}^1 \hookrightarrow \mathbb{S}^3 \xrightarrow{\pi} \mathbb{S}^2,$$

where $\mathbb{S}^3$ is the total space, $\mathbb{S}^2$ the base space, $\mathbb{S}^1$ the fiber space, and $\pi : \mathbb{S}^3 \longrightarrow \mathbb{S}^2$, the so-called Hopf map, the bundle projection.

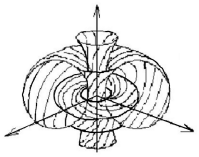

Figure 2. The Hopf fibration.

The Hopf fibration, like any fiber bundle, has the important property of local triviality, (looks locally as a product), however it is not a trivial fiber bundle, that is, $\mathbb{S}^3$ is not globally equal to $\mathbb{S}^3 \times \mathbb{S}^2$. Hopf fibration provides a basic example of a principal bundle by identifying the fiber with the circle group.

Stereographic projection of the Hopf fibration induces a remarkable structure on the space $\mathbb{R}^3$, it turns out that the space is filled with nested tori made of linking *Villarceau circles*. Each fiber projects to a circle in space, including the circle through infinity, and each torus is the stereographic projection of the inverse image of a circle of latitude of $\mathbb{S}^2$. For details we refer the reader to the volume by G.L. Naber [G.L. Naber, 2000], and the beautiful paper by H.K. Urbantke [H.K. Urbantke, 2003]. Figure 2 illustrates the well know picture of the Hopf fibration.

Now from equations (12) and (13) we introduce the following the two complex variables

$$\begin{aligned}
z_1 &= \omega_0\sqrt{m/2H}\, u, \\
z_2 &= \sqrt{m/2H}\, \dot{u}.
\end{aligned}$$

For then, the dynamics develops on $\mathbb{S}^3$ given by the conservation of energy (14) that now is written as

$$|z_1|^2 + |z_2|^2 = 1.$$

Now, by means of Hopf map $\pi : \mathbb{S}^3 \to \mathbb{CP}^1 = \mathbb{S}^2$, the 2-sphere $\mathbb{S}^2$ is described by the unit vector $\hat{n} = (n_1, n_2, n_3)$ with components

$$\begin{aligned}
n_1 &= 2\mathrm{Re}(z_1 z_2^*), \\
n_2 &= 2\mathrm{Im}(z_1 z_2^*), \\
n_3 &= |z_1|^2 - |z_2|^2,
\end{aligned}$$

satisfying

$$n_1^2 + n_2^2 + n_3^2 = 1.$$

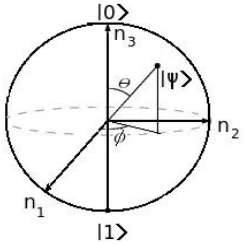

Figure 3. The Bloch sphere.

This surface is known as *Bloch sphere* in the study of two level systems, of nuclear magnetic resonance, nonlinear optics and quantum computing. The points on the sphere correspond to the *pure states* $|\psi\rangle$ of the system, whereas the points in the interior correspond to *mixed states*. Each pair of antipodal points correspond to mutually orthogonal state vectors, the north and south poles are customarily chosen to correspond to the standard basis vectors $|0\rangle$ and $|1\rangle$, respectively, which in turn might correspond to the spin-up and spin-down states of an electron, see figure 3.

Observe that the sets of points $z_0 z_1$ and $z_0 z_2$ for $|z_0| = 1$ are circles through z_1 respectively through z_2 and are mapped to the same point on $\mathbb{S}^2$.

As mentioned before, the fiber bundle structure is given by $\mathbb{S}^1 \hookrightarrow \mathbb{S}^3 \xrightarrow{\pi} \mathbb{S}^2$ where $\mathbb{S}^3$ is the total space, $\mathbb{S}^2$ the base space, $\mathbb{S}^1$ the fiber space and π the projection. In our problem to multiply z_1, respectively z_2, by a unit complex number is equivalent to rotate the plane $\{x_1, x_2\}$.

Since the solution is a rotation by an angle $\tilde{\omega}t$ of an ellipse parameterized by an angle $\tilde{\omega}_0 t$, we conclude that, all arcs of trajectories in base space, which can be obtained by a rotation from a given one, are mapped to the same curve on $\mathbb{S}^2$ by the Hopf map. The resulting curve will be thus the same for all *equivalent* arcs. The Bloch vector $\hat{n}$ satisfies

$$\frac{d\hat{n}}{dt} = \vec{\Omega} \times \hat{n}, \tag{15}$$

with constant angular velocity $\vec{\Omega} = (0,\, -2\omega_0,\, 2\tilde{\omega})$.

The canonical angular momentum conservation leads to the planes

$$-\omega_0 n_2 + \tilde{\omega} n_3 = \frac{1}{2}\vec{\Omega} \cdot \hat{n} = \frac{\omega_0^2\, L_z}{H} - \tilde{\omega}.$$

They are at a distance $(\omega_0^2 L_z - H\tilde{\omega})/(H\tilde{\omega}_0)$ from the origin, their normal unit vectors are $(0, -\omega_0/\tilde{\omega}_0, \tilde{\omega}/\tilde{\omega}_0) = \vec{\Omega}/\Omega$ and the intersections of these planes with $\mathbb{S}^2$ are of course circles. In the case for which $H = mR^2\omega_0^2/2$ we have

$$\hat{n} = (-\frac{\omega_0}{\tilde{\omega}_0}\sin(2\tilde{\omega}_0 t), \frac{\omega_0(-\tilde{\omega} + \tilde{\omega}\cos(2\tilde{\omega}_0\, t))}{\tilde{\omega}_0^2}, \frac{\tilde{\omega}^2 + \omega_0^2\cos(2\tilde{\omega}_0\, t)}{\tilde{\omega}_0^2}).$$

The two halves of the spheres are foliated by circles independent of the initial position R or the energy. The circles on one half are for $\tilde{\omega}/\omega_0 > 0$ and on the other half for $\tilde{\omega}/\omega_0 < 0$. All circles pass through the north pole. The isolated north pole also corresponds to the limit cases where the ratio of the frequencies is $\pm$ infinity, associated to the Heisenberg flywheel or a charged particle in a perpendicular static magnetic field. When $\tilde{\omega}/\omega_0 = 0$ the circles become a meridian that corresponds to a two dimensional harmonic oscillator. For $\tilde{\omega}/\omega_0 = \pm 1$ two circles connect the north pole with the equator. Finally, each circle corresponds to a single curve arch in the base space $\{x_1, x_2\}$ trajectory traversed in half a period. For the general case $H = mx_0^2\omega_0^2/2 + mv_0^2/2$ and $L_z = mx_0 v_0 \sin(\beta) + m\tilde{\omega}x_0^2$. The components of the normal vector are

$$\begin{aligned}
n_1 &= \frac{m\omega_0}{2H\tilde{\omega}_0}(2\tilde{\omega}_0 v_0 x_0 \cos(\beta)\cos(2\tilde{\omega}_0 t) \\
&\quad + [v_0^2 - \omega_0^2 x_0^2 + 2\tilde{\omega}v_0 x_0 \sin(\beta)]\sin(2\tilde{\omega}_0 t)), \\
n_2 &= \frac{m\omega_0}{2H\tilde{\omega}_0^2}(\tilde{\omega}v_0^2 - \tilde{\omega}\omega_0^2 x_0^2 - 2\omega_0^2 v_0 x_0 \sin(\beta) \\
&\quad - \tilde{\omega}\cos(2\tilde{\omega}_0 t)[v_0^2 - \omega_0^2 x_0^2 + 2\tilde{\omega}v_0 x_0 \sin(\beta)] \\
&\quad + 2\tilde{\omega}\tilde{\omega}_0 v_0 x_0 \cos(\beta)\sin(2\tilde{\omega}_0 t)) \\
n_3 &= \frac{m}{2H\tilde{\omega}_0^2}\Big(-\tilde{\omega}^2 v_0^2 + \omega_0^2\tilde{\omega}^2 x_0^2 + 2\omega_0^2\tilde{\omega}v_0 x_0 \sin(\beta) \\
&\quad - \omega_0^2\cos(2\tilde{\omega}_0 t)[v_0^2 - \omega_0^2 x_0^2 + 2\tilde{\omega}v_0 x_0 \sin(\beta)] \\
&\quad + 2\omega_0^2\tilde{\omega}_0 v_0 x_0 \cos(\beta)\sin(2\tilde{\omega}_0 t)).
\end{aligned}$$

Again, the conservation of the canonical angular momentum leads to circular trajectories around the vector $\vec{\Omega}$.

For $\tilde{\omega} = 0$, uncoupled harmonic oscillator, the coordinate n_2 is constant and the corresponding limit circle is perpendicular to the $\{n_1, n_2\}$ plane and separates the sphere in two unequal parts in general. The limit case $\omega_0 = 0$ is the south pole for $v_0 \neq 0$, since then $n_3 = -1$, and the north pole for $v_0 = 0$ and $x_0 \neq 0$ which lead to $n_3 = 1$.

Perform now a rotation such that the angular velocity $\vec{\Omega}$ coincides with the n_3 axis, i.e., introduce the coordinates $n_1' = n_1, n_2' = \tilde{\omega}n_2/\tilde{\omega}_0 + \omega_0 n_3/\tilde{\omega}_0$ and $n_3' = -\omega_0\, n_2/\tilde{\omega}_0 + \tilde{\omega}n_3/\tilde{\omega}_0$. More explicitly

$$\begin{aligned}
n_2' &= \frac{m\omega_0}{2H\tilde{\omega}_0}(-[v_0^2 - \omega_0^2 x_0^2 + 2\tilde{\omega}v_0 x_0 \sin(\beta)]\cos(2\tilde{\omega}_0 t) \\
&\quad + 2\tilde{\omega}_0 v_0 x_0 \cos(\beta)\sin(2\tilde{\omega}_0 t)).
\end{aligned}$$

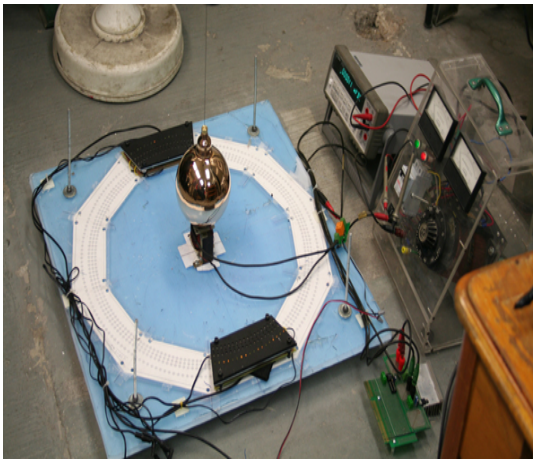

Figure 4. The Foucault Pendulum at UAM-A.

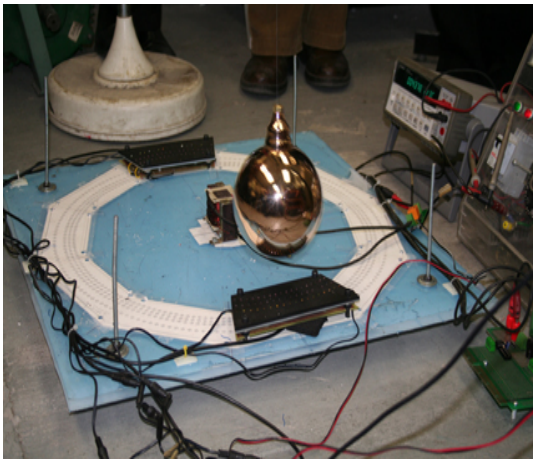

Figure 5. The closed loop scheme for the Foucault Pendulum at UAM-A.

The coordinate n_3' is the constant $(\omega_0^2 L_z - \tilde{\omega} H)/(H\tilde{\omega}_0)$ and (n_1', n_2') describes a circle centered on the n_3' axis.

Further geometrical analysis shall be carried out somewhere else for exploiting the richness of the Hopf fibration in the same spirit of the aforementioned reference of H.K. Urbantke.

5 Conclusion and research perspectives

We formulate the classical Foucault pendulum in the framework of geometric optimal control theory, the small oscillation consideration allow to reduce the state manifold to the three dimensional Heisenberg group. The Pontryagin Maximum Principle yields the optimal controls that in turn allow to write explicitly the solutions. With these expressions at hand we establish an intriguing connection with the well known Hopf fibration, that open an interesting line of theoretical research.

Appendix

One of the motivations for studying theoretical aspects of the Foucault pendulum was the involvement of the authors in the the project of installation of a real Foucault pendulum at the UAM-Azcapotzalco in México City. The project is now at the level of a prototype design that we shall briefly describe.

5.1 Physical Characteristics

It consist of a perfect 10 kilograms bronze (SAE 65) sphere with a central cylindrical axis of 1in of diameter of stainless steel (SW 10), perfectly coupled to the sphere. This ferromagnetic composition allows the action of electromagnetic devices. The sphere is suspended by a iron cable of seven threads of type $(1 \times 7 + 0)$, see figure 4.

The pendulum is initialized as in the original experiment from rest and is energized by mean of an electromagnetic impulse on the bottom by means of a coil that energizes the pendulum on a regular basis. The electromagnetic force was calculated by means of a COMSOL Multiphysics 3.5's simulation for a permanent oscillation of $5°$, see table 2.

$1°$	$2°$	$3°$	$4°$	$5°$
-1.1 E08	4.2 E07	1.3 E07	-9.8 E10	4.2 E10
7.4 E06	-6.8 E06	-3.9 E05	-1.9 E06	-2.9. E07
-5.0 E04	-5.4 E04	-1.2 E05	-2.8 E07	-5.8 E08
5.0 E04	5.4 E04	4.1 E05	2.0 E06	2.9 E07

Table 2. Estimation of the electromagnetic impulse.

5.2 The control and vision system

It consist of three fundamental parts, namely, a three rings circular configuration of eight independent modules of sensors. An interactive mechanism with a central controller of each module and a web cam. The permanent communication of the modules determines a closed loop scheme where feedback is generated by infrared presence sensors that triggers the electromagnetic impulse within a determined threshold, see figure 5.

The web cam has a fix IP and interfaces with the central controller for keeping track of the movement, for generating data regarding position, velocity and acceleration, as well as database of images that can be used for image reconstruction experiments, see figure 6.

References

C. Lobry (1970), Contrôlabilité des systèmes non linéaires, *SIAM J. Control*, 8.

R.W.Brockett (1972), System theory on group manifolds and coset spaces, *SIAM J. Control*, 10.

V. Jurdjevic, H.J. Sussmann (1972), Control systems on Lie groups, *J. Differential Equations*, 12.

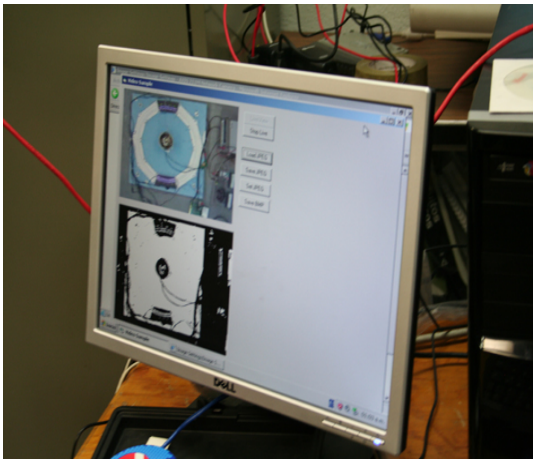

Figure 6. Control and vision system.

F. Bullo and A.D. Lewis (2004), Geometric Control of Mechanical Systems, Texts in Applied Mathematics, Springer.

R. Murray, L. Zexiang,S.S. Sastry (1994), A mathematical introduction to robotic manipulation, CRC Press.

V. Jurdjevic (1997), Geometric control theory, Cambridge studies in advanced mathematics 51, Cambridge University Press .

A. Agrachev, Y.L. Sachkov (2004), Control theory from the geometric viewpoint. Encyclopaedia of Mathematical Sciences, 87. Control Theory and Optimization, II. Springer-Verlag, Berlin.

L.S. Pontryagin, V.G. Boltyanskii, R.V. Gamkrelidze; E.F. Mishchenko (1962), The mathematical theory of optimal processes edited by L. W. Neustadt Interscience Publishers John Wiley & Sons, Inc. New York-London.

M. Giaquinta, S. Hildebrandt (1996), Calculus of variations. I. The Lagrangian formalism. Grundlehren der Mathematischen Wissenschaften [Fundamental Principles of Mathematical Sciences], 310. Springer-Verlag, Berlin.

A.M. Vershik and V. Ya. Gershkovich (1991), Nonholonomic dynamical systems, geometry of distributions and variational problems, in *Encyclopaedia of Mathematical Sciences, Vol. 16; Dynamical systems VII*, V.I. Arnold and S.P. Novikov eds., Springer-Verlag.

R. Montgomery (2002), A tour of subriemannian geometries, their geodesics and applications, Mathematical surveys and monographs, Vol. 91, American Mathematical Society.

O. Calin, D.Ch. Chang (2009), Sub-Riemannian Geometry General Theory and Examples, Encyclopedia of Mathematics and its Applications No. 126, Cambridge University Press.

A. Anzaldo-Menenses and F. Monroy-Pérez (2010), *J. math. Phys.*, **51**, 082703.

A.Anzaldo-Meneses and F. Monroy-Pérez (2009), *Sub-Riemannian approach for the Foucault pendulum*, PHYSCON 2009, Catania, Italy.

Heinz Hopf (1931), Über die Abbildungen der dreidimensionalen Sphäre auf die Kugelfläche, *Mathematische Annalen*,Springer 104 (1): 637665, Berlin. doi:10.1007/BF01457962, ISSN 0025-5831

G.L. Naber (2000), Topology, geometry and gauge fields, Interactions, Applied Mathematical Sciences 141, Springer-Verlag, New-York.

H.K. Urbantke (2003), The Hopf fibration– seven times in physics, *Journal of Geometry and Physics*, 46,125–150.